PERGAMON

International Journal of Solids and Structures 36 (1999) 669–695

INTERNATIONAL JOURNAL OF SOLIDS and STRUCTURES

Phenomenological modeling of the non-linear electro-mechanical coupling in ferroelectrics☆

Marc Kamlah*, Charalampos Tsakmakis

Forschungszentrum Karlsruhe GmbH, Institut für Materialforschung II, Postfach 3640, D-76021 Karlsruhe, Germany

Received 15 February 1997; in revised form 26 January 1998

Abstract

Our objective is the construction of a phenomenological model of ferroelectricity for general electro-mechanical loading histories, which is simple enough to be implemented in an FE-code with realistic effort. In this paper we motivate and verify the one-dimensional formulation of such a model. It relies upon introducing the remanent polarization and the remanent strain as internal variables besides stress, strain, electric field and polarization. The internal variables are governed by ordinary differential equations. Each of these evolution equations is subjected to two loading conditions of different nature. The first one indicates the onset of changes of the remanent quantities by domain switching, while the second one characterizes the saturation value of a remanent quantity corresponding to a totally switched domain structure. Polarization induced anisotropy is taken into account as far as it seemed necessary. For simplicity, no rate effects are included.

The model response to uniaxial electro-mechanical loading histories will be discussed in comparison to known experimental results. By means of a bilinear approximation the following characteristic phenomena of macroscopic ferroelectricity are represented: dielectric hysteresis, polarization induced piezoelectricity, butterfly hysteresis, ferroelastic hysteresis, mechanical depolarization.

1. Introduction

Since the piezoelectric effect causes a coupling between electric and mechanical fields, it is of high interest for advanced sensor and actuator applications in so-called intelligent systems. In many cases, the piezoelectric effect is realized by the ferroelectric phase of certain lead zirconate titanate ceramics (PZT). If such a material has been poled by an electric field above the coercitive field at a temperature below the Curie point, its response to small signals may be characterized by

* Corresponding author. Tel.: (+49)7247/825860; fax: (+49)7247/822347; e-mail: marc.kamlah@imf.fzk.de.

☆ Dedicated to Professor Dr D. Munz on the occasion of his 60th birthday.

0020–7683/99/$ - see front matter
PII: S0020–7683(98)00040–7

the parameters of classical linear piezoelectricity. However, nowadays applications involve severe loadings and complicated geometries such that the assumption of small signals is no longer justified in general. Rather, the non-linear behavior of the material may become dominant.

In order to assess the reliability of a PZT-component, it is important to have as precise knowledge of the mechanical stress state as possible. For this purpose, the electric and mechanical field equations have to be solved for the case of an appropriate phenomenological constitutive model. This may be done by means of the finite element method, as soon as a model is available, which takes into account the characteristic, non-linearly coupled phenomena of macroscopic ferroelectricity. However, in searching the scientific literature we were not able to find such a nonlinear model that would be ready for implementation in an FE-Code.

Obviously, this point needs further discussion and thus we will present a short summary of related previous work in the next section. In Section 3, we present the structure of our phenomenological model in a three-dimensional formulation and give its one-dimensional specialization. In particular, we introduce certain internal variables representing the history dependence of the irreversible material behavior. Some well-known microscopic interpretations of typical macroscopic phenomena are summarized in Section 4. Finally, the one-dimensional evolution laws of the internal variables are motivated in two steps in Sections 5 and 6, and the resulting model response is discussed in Section 7.

In the following analysis, all component representations of tensors are referred to a Cartesian coordinate system (summation convention). First-order tensors (vectors) are denoted by upright letters with superscript arrows ($\vec{\mathrm{a}}, \vec{\mathrm{A}}$) and second-order tensors (tensors) by bold slanted letters ($\boldsymbol{a}, \boldsymbol{A}, \boldsymbol{\alpha}$). A dot between tensors indicates the contraction relative to one index, for example, the inner product between vectors, i.e. $\vec{\mathrm{a}} \cdot \vec{\mathrm{b}} = \mathrm{a}_i \mathrm{b}_i$, the composition of two tensors, i.e. $\boldsymbol{A} \cdot \boldsymbol{A}^{-1} = \boldsymbol{I}$ ($\boldsymbol{A}^{-1}$: inverse of $\boldsymbol{A}$, $\boldsymbol{I}$: identity tensor), the inner product between tensors, i.e. $\boldsymbol{A} : \boldsymbol{B} = \mathrm{tr}(\boldsymbol{A} \cdot \boldsymbol{B}^T) = A_{ij} B_{ij}$ ($\mathrm{tr}\,\boldsymbol{A}$: trace of $\boldsymbol{A}$, $\boldsymbol{B}^T$: transpose of $\boldsymbol{B}$), the linear mapping of a vector by a tensor, i.e. $\boldsymbol{A} \cdot \vec{\mathrm{a}} = A_{ij} \mathrm{a}_j$. $\boldsymbol{A}^D = \boldsymbol{A} - \frac{1}{3}(\mathrm{tr}\,\boldsymbol{A})\boldsymbol{I}$ stands for the deviator of $\boldsymbol{A}$ and $\|\boldsymbol{A}\| = \sqrt{\boldsymbol{A} : \boldsymbol{A}}$ is the norm of the tensor $\boldsymbol{A}$. $\vec{\mathrm{e}}_\mathrm{a} = \vec{\mathrm{a}}/\|\vec{\mathrm{a}}\|$ is the unit vector in the direction of the vector $\vec{\mathrm{a}}$ ($\|\vec{\mathrm{a}}\| = \sqrt{\vec{\mathrm{a}} \cdot \vec{\mathrm{a}}}$: norm of $\vec{\mathrm{a}}$). The symbol $\otimes$ indicates the dyadic product, e.g. $\vec{\mathrm{a}} \otimes \vec{\mathrm{b}}$ yields a second order tensor with components $\mathrm{a}_i \mathrm{b}_j$. $\dot{(\,)} = \mathrm{d}(\,)/\mathrm{d}t$ denotes the time derivative of a field $(\,)$. Further mathematical definitions will be given where they are needed.

Concerning the physics relevant for this paper, we expect the reader to have some basic knowledge of piezoelectricity and ferroelectricity. For introductory literature we refer to the next section. With respect to our subject, we may recommend the instructive works Hao et al. (1996), Jiang (1995), and Schäufele (1996).

2. On related previous work

In this section, we discuss experimental data found in the literature, which may serve as a basis for constructing a phenomenological model. Furthermore, we discuss some papers with respect to the goal of developing a macroscopic model of ferroelectricity.

2.1. Experimental investigation of material behavior

In text books and review articles, one may find curves characterizing piezoelectricity and ferroelectricity, e.g. Fatuzzo and Merz (1967), Jaffe et al. (1971), Zheludev (1971), Feldtkeller

(1973), and Haertling (1987). The purpose of these curves is in the first place to demonstrate the ferroelectric non-linearities and the underlying physical mechanisms as well as characterizing chemical compositions. However, for the development of a phenomenological model describing ferroelectric non-linearities and couplings within a continuum theory, such curves are not sufficient.

The characterization of the linear range of electro-active ceramics, i.e. the measurement of the classical piezoelectric constants has been standardized for a long time (e.g. IRE, 1958). For the non-linear range of ferroelectric materials the situation is quite different. Systematic experimental work on the determination of the non-linear phenomenological behavior of polycrystalline ferroelectric ceramics is rare. One may find (e.g. in Haertling, 1987) some parameters describing limiting states as the coercitive field or the maximum remanent polarization. Chen and Tucker (1981) identified the typical dielectric and butterfly hystereses as equilibrium properties in the sense that they are present even under vanishing rate of loading.

Cao and Evans (1993) and Schäufele (1996) are pioneering works in the field of the experimental investigation of the ferroelectric coupling (see also Lynch, 1996; Schäufele and Härdtl, 1996). At different PZT-materials uniaxial loadings have been realized by applying uniaxial mechanical pressure and an electric field. Two different groups of plots have been recorded which are typical of ferroelectric ceramics. First, the plot of stress over strain shows the 'ferroelastic' ('pseudo-plastic') hysteresis. Second, the depolarization of the material under mechanical compression loading could be demonstrated. The recorded macroscopic curves were interpreted successfully as a consequence of microscopic domain switching processes. This interpretation was supported by proving the inelastic part of the deformation to be volume preserving.

2.2. Macroscopic description of ferroelectricity

A macroscopic continuum theory consists of two classes of equations. The first class is given by a system of partial differential equations being derived from the universal balance laws for all material bodies. This system of field equations has to be closed by the second class of equations representing the individual properties of the material under consideration.

In the case of a deformable dielectric body, the field equations are given in general by the balance laws of thermomechanics and Maxwell's equations of electrodynamics (see Truesdell and Noll, 1965; Landau and Lifschitz, 1967). For technical applications, the strains are expected to be much smaller than 5% and thus, it will be justified to restrict oneself to the geometrical linear case. Furthermore, the material velocities considered will not exceed the order of magnitude of acoustical velocities of propagation. Under these conditions, the quasi-electrostatic approximation applies, i.e. the system of field equations for deformable dielectric bodies reduces (in the isothermal case) to the balance of linear momentum and Gauss' law for the electric displacement (see Maugin, 1988).

In contrast to the field equations, the phenomenological constitutive modeling is still an open research area. Of course, an important exception is given by Voigt's classical theory of linear piezoelectricity, which is discussed e.g. in Maugin (1988), Maugin et al. (1992), and Parton and Kudryavtsev (1988) in detail (cf also Toupin, 1956). The non-linear ferroelectric material response shows hystereses and rate effects. Thus the material response depends on the loading history and cannot be represented by simply adding to the constitutive functions of linear piezoelectricity some non-linear terms.

As it seems, this finding has been realized for the first time by Chen and coworkers for a phenomenological model of ferroelectricity (e.g. Chen and Peercy, 1979; Chen and Marsden, 1981). At the beginning, the model was formulated uniaxially and covered essentially the loading by an electric field. The history and rate dependence of the model response was implemented by introducing internal variables with ordinary differential equations as evolution laws. The dielectric and butterfly hystereses were well represented. However, even though the model does not cover further electro-mechanical coupling phenomena it became quite involved. Chen (1980) proposed a general structure for a three-dimensional theory but explicit equations were not given. The model seems not to have been developed further (Chen, 1984).

Another attempt to describe macroscopic ferroelectricity has been made by Bassiouny et al. (1988), Bassiouny and Maugin (1989). Their model was constructed by transferring concepts of elasto-plasticity and of the phenomenological description of ferromagnetism. The resulting thermodynamic theory makes use of plastic deformation and remanent polarization as internal variables. With the help of a dissipation potential, evolution equations subjected to loading conditions were derived. This general model structure seems to be promising. However, it was not elaborated further by the authors to a model ready for application (cf Chapter 6 in Maugin et al. 1992).

More recently, it has been tried to simulate macroscopic ferroelectricity on the basis of microscopic models for the behavior of single domains. Hwang et al. (1995) simulated numerically a model consisting of 10,000 randomly oriented grains, where each grain shows an idealized rectangular hysteresis for the dielectric behavior. With the help of an energetically motivated criterion for domain switching caused by an electric field or mechanical stress, the macroscopic dielectric and butterfly hystereses where described. Loge and Suo (1996) developed a theory of the movement of domain walls in polydomain ferroelectrics by analogy to the theory of grain growth. Under the action of generalized forces, domain walls move in a thermodynamic non-equilibrium process such that an energetic variational functional is minimized. Huo and Jiang (1995) employed a continuum mixture approach, where each domain is associated to a phase (constituent). Domain switching corresponds to phase change processes, which are subjected to an energetic switching criterion leading to a hysteretic behavior. Even though these approaches are appealing because of their well sound physical basis, it is not yet clear whether they will lead to models suitable for engineering applications.

In a very recent and interesting work Michelitsch and Kreher (1996) follow a similar approach as Hwang et al. (1995). The model describes the averaged behavior of a polydomain ferroelectric under the action of electric and mechanical loads being subjected to an energetic switching criterion. The key assumption is that each single grain is transversely isotropic (instead of being tetragonally isotropic) and as a consequence, macroscopic constitutive behavior is derived analytically from microscopic assumptions. The first polarization curve starting from an isotropic orientation distribution function is calculated as well as the stable dielectric hysteresis loop. Furthermore, expressions for the dependence of the spontaneous strain and the piezoelectric moduli on the polarization are given. Depolarization induced by mechanical loading is considered, too. The model is still in the development stage.

Significantly less complex than ferroelectricity is the electro-mechanical coupling caused by electrostriction. In principle, this phenomenon is present in materials with arbitrary symmetry groups, i.e. with and without a center of symmetry in their unit cell. However, electrostriction is

an effect of second order which is dominated in materials possessing the appropriate material symmetry by their piezoelectricity. Nevertheless, considering electrostriction turned out to be useful, because meanwhile exist materials exhibiting a technically exploitable extend of electro-mechanical coupling which might be described as electrostriction. Besides, ferroelectric ceramics show above the Curie temperature in their paraelectric phase only electrostrictive behavior. (For the description of load induced phase changes in ferroelectric see Jiang, 1995.)

The recent papers Suo (1991), Hom and Shankar (1994), Yang and Suo (1994), and Hao et al. (1996) present two successful attempts to describe electrostrictive coupling by means of thermodynamically based phenomenological models. The models are non-linear in the sense that the electrostrictive strain depends quadratically on the polarization and the dielectric curve becomes stationary for large values of the electric field. The models employ no internal variables with differential equations as evolution laws. Rather they consist of non-linear constitutive functions only, thereby expressing that the material response is independent of the loading history. Assuming isotropy, which seems to be justified in the case of the paraelectric phase, allows immediate generalization to a three-dimensional model.

The implementation of a non-linear constitutive model in an electro-mechanical FE-Code is not as involved for models restricted to non-linear response functions (cf Gaudenzi and Bathe, 1995) as it would be if the model would make use of differential equations. In the sense of this restricted nonlinearity, the model of Suo (1991) has been exploited for electro-mechanically coupled, non-linear FE-analyses (Gong, 1995; Gong and Suo, 1996a,b). In an electrostrictive multilayer actuator, critical areas with tensile stresses were detected. The electrostrictive saturation strain and Young's modulus turned out to be important parameters. For the comparable weak electrostrictive coupling, the influence of the mechanical stress on the electric quantities appeared to be negligable.

3. The general structure of the model

As mentioned before, a macroscopic theory of a deformable dielectric body is (in absence of body forces and external body charges) based on the balance of linear momentum,

$$\rho\ddot{\vec{u}} = \operatorname{div} \boldsymbol{T} \tag{1}$$

($\vec{u}$, $\boldsymbol{T}$, ρ: displacement vector, stress tensor, mass density, respectively) and Gauss law,

$$\operatorname{div} \vec{D} = 0. \tag{2}$$

This system needs to be closed by a macroscopic constitutive law relating the stress tensor and the electric field $\vec{E} = -\operatorname{grad}\phi$ to the strain tensor $\boldsymbol{E} = \frac{1}{2}(\operatorname{grad}\vec{u} + (\operatorname{grad}\vec{u})^T)$ and the polarization $\vec{P} = \vec{D} - \epsilon_0\vec{E}$ (ϕ, ϵ_0: electric potential, dielectric constant of vacuum, respectively):

$$\left.\begin{matrix}\boldsymbol{T}\\ \vec{E}\end{matrix}\right\} \leftrightarrow \left\{\begin{matrix}\boldsymbol{E}\\ \vec{P}\end{matrix}\right. \tag{3}$$

The key assumption of our approach is to introduce the internal or remanent polarization $\vec{P}^{in}$ and the internal or remanent strain $\boldsymbol{E}^{in}$ as independent internal variables in order to catch the history dependence of the material response. We define these internal variables by the additive decompositions of the polarization

$$\vec{P} = \vec{P}^{rv} + \vec{P}^{in} \tag{4}$$

and the strain

$$\boldsymbol{E} = \boldsymbol{E}^{rv} + \boldsymbol{E}^{in} \tag{5}$$

respectively (cf Bassiouny et al., 1988; Bassiouny and Maugin, 1989), for a thermodynamical motivation of these additive decompositions). The polarization vector $\vec{P}^{rv}$ and the strain tensor $\boldsymbol{E}^{rv}$ are called reversible in the sense that they are assumed to vanish with vanishing external loads (e.g. mechanical stress or electric field).

For $\vec{P}^{in}$ and $\boldsymbol{E}^{in}$, evolution laws reflecting the history dependence of the material response will be motivated later on. In order to present our concepts in a format which is as simple as possible, we will introduce the evolution laws in a one-dimensional formulation. However, for the time being we continue with the three-dimensional formulation of the theory for two reasons: first, for the motivation of our choice of the internal variables it is necessary to take into account their tensorial rank (see Section 3.1). Second, only a tensorial framework allows it to discuss history dependent anisotropy properties appropriately (see Section 3.2).

3.1. Representation of irreversible changes

A ferroelectric is a polycrystal, where the lattice structure of a single grain might, for example, be thought of to possess tetragonal symmetry. In this case, each unit cell within the lattice has a brick-like geometry with the dimensions $a \times a \times c$, where $c > a$. The relative displacement along the c-axis of the centers of positive and negative charges of this unit cell constitutes its microscopic spontaneous polarization. A region within a grain of equal spontaneous polarization is called domain.

In the unpoled state, the orientation of the spontaneous polarization is distributed randomly, i.e. isotropically, and the ferroelectric has no macroscopic polarization. Under the action of sufficiently strong electric fields or mechanical stresses, the orientation of the spontaneous polarization can be switched. This will result in irreversible changes of the macroscopic strain and the macroscopic polarization, respectively (see Fig. 1).

On the microscopic level, the spontaneous polarization and the spontaneous strain of a single domain are strictly related to each other. For instance, for a tetragonal unit cell, the axis of the spontaneous polarization is equal to the c-axis, i.e. the direction of its elongation relative to the cubic state. Furthermore, the amount of the elongation depends on the magnitude of spontaneous polarization. (From solid state physics, this dependence is known to be quadratic.) However, as will be discussed in the following, in our macroscopic approach the remanent polarization $\vec{P}^{in}$ and the remanent strain $\boldsymbol{E}^{in}$ have to be considered as independent quantities.

The macroscopic internal variables $\vec{P}^{in}$ and $\boldsymbol{E}^{in}$ must be understood as averages of the corresponding microscopic quantities. In particular, the remanent polarization $\vec{P}^{in}$ does not indicate whether a material is in its ferroelectric phase with polarized domains. Rather, it stands for the net polarization of a neighborhood of many polarized domains with possibly different orientations. It has to be looked at as a measure for the extent of the alignment and orientation of the domains in a certain direction.

In view of these properties, the remanent polarization $\vec{P}^{in}$ may be related to a residual strain of

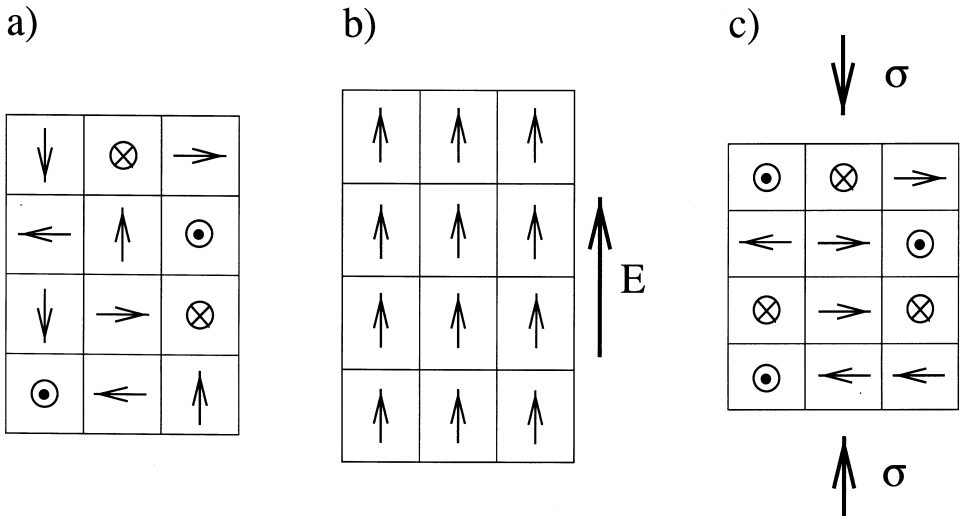

Fig. 1. Symbolic representation of switching mechanisms in a ferroelectric ceramic: each brick stands for a unit cell, the arrow indicating its spontaneous polarization. (a) Vanishing initial macroscopic polarization. (b) Fully poled domain structure for $E > E_c$. (c) Depolarization and remanent deformation by a compressive stress.

the above mentioned neighborhood representing the net deformation caused by the alignment of domains in the direction of poling (compare Fig. 1(a) to Fig. 1(b)). We denote this part of the remanent strain by $\boldsymbol{E}^{\mathrm{P}}$ and call it strain induced by the remanent polarization. Since it represents the consequences of domain reorientation on the strain state, it seemed appropriate to us to assume $\boldsymbol{E}^{\mathrm{P}}$ to be isochoric, and we introduce the deviatoric strain tensor

$$\boldsymbol{E}^{\mathrm{P}} = \frac{3}{2}\varepsilon_{\mathrm{sat}}\frac{\|\vec{\mathrm{P}}^{\mathrm{in}}\|}{\mathrm{P}_{\mathrm{sat}}}\left(\vec{\mathrm{e}}_{\mathrm{P}^{\mathrm{in}}} \otimes \vec{\mathrm{e}}_{\mathrm{P}^{\mathrm{in}}} - \frac{1}{3}\boldsymbol{I}\right). \tag{6}$$

$\boldsymbol{E}^{\mathrm{P}}$ yields a uniaxial strain state with an elongation by $\|\vec{\mathrm{P}}^{\mathrm{in}}\|\varepsilon_{\mathrm{sat}}/\mathrm{P}_{\mathrm{sat}}$ along the direction of poling and a contraction of half amount perpendicular to it. In this equation, the saturation polarization $\mathrm{P}_{\mathrm{sat}}$ is the maximum value of the magnitude of the remanent polarization in the fully poled state: $\|\vec{\mathrm{P}}^{\mathrm{in}}\| \leqslant \mathrm{P}_{\mathrm{sat}}$. The saturation strain $\varepsilon_{\mathrm{sat}}$ is the maximum remanent elongation corresponding to the fully poled state ($\|\vec{\mathrm{P}}^{\mathrm{in}}\| = \mathrm{P}_{\mathrm{sat}}$).

The material constant $\mathrm{P}_{\mathrm{sat}}$ is not to be understood as the microscopic spontaneous polarization of a single domain. Rather it represents the maximum magnitude of the macroscopic remanent polarization obtained by averaging over a certain region (cf Hwang et al., 1995). In general, this saturation polarization will be lower than the spontaneous polarization of a single domain, since it is unlikely that the domains of different grains can be aligned completely in the same direction.

It is well known, that a polydomain ferroelectric may suffer ferroelastic deformation from mechanical loading (Cao and Evans, 1993; Schäufele, 1996). The mechanical stress may switch domains, but it is not able to give preference to a unique orientation of domains in a particular direction, i.e. a net polarization. (Rather, comparing Fig. 1(b) to Fig. 1(c) we seen that the spontaneous polarizations of mechanically switched domains cancel each other out, resulting in

the phenomenon of depolarization.) Consequently, we have to consider additionally a ferroelastic part of the remanent strain,

$$\boldsymbol{E}^{\mathrm{f}} = \boldsymbol{E}^{\mathrm{in}} - \boldsymbol{E}^{\mathrm{P}}. \tag{7}$$

$\boldsymbol{E}^{\mathrm{f}}$ has to be deviatoric, because it results from domain switching as well. Note that eqn (7) must not be understood in the sense that the influence of electric and mechanical loads on the remanent strain can be decomposed linearly. For instance, $\boldsymbol{E}^{\mathrm{P}}$ will change with electrically and mechanically caused changes of the remanent polarization $\vec{\mathrm{P}}^{\mathrm{in}}$. For further discussion of this point we refer to Sections 6.2 and 6.3.

From the above considerations we conclude that $\vec{\mathrm{P}}^{\mathrm{in}}$ and $\boldsymbol{E}^{\mathrm{f}}$ are independent state variables (besides an external electric ($\vec{\mathrm{P}}$ or $\vec{\mathrm{E}}$) and mechanical ($\boldsymbol{E}$ or $\boldsymbol{T}$) variable). In view of eqns (6) and (7) follows mathematically our previous statement about the independence $\vec{\mathrm{P}}^{\mathrm{in}}$ and $\boldsymbol{E}^{\mathrm{in}}$. This means that evolution laws are needed for either one of these pairs ($\vec{\mathrm{P}}^{\mathrm{in}}, \boldsymbol{E}^{\mathrm{in}}$) and ($\vec{\mathrm{P}}^{\mathrm{in}}, \boldsymbol{E}^{\mathrm{f}}$). As can be seen in the next sections, we prefer the latter.

3.2. Representation of reversible changes

The reversible parts $\vec{\mathrm{P}}^{\mathrm{rv}}$ and $\boldsymbol{E}^{\mathrm{rv}}$ arising by the above decompositions of $\vec{\mathrm{P}}$ and $\boldsymbol{E}$ may be related to the stress and the electric field such that they represent the linear piezoelectric contribution to the material behavior of a ferroelectric. For the reversible part of the polarization we choose

$$\vec{\mathrm{P}}^{\mathrm{rv}} = \mathbb{d} : \boldsymbol{T} + \epsilon \cdot \vec{\mathrm{E}} \tag{8}$$

where ϵ is the (second-order) tensor of dielectric permittivities and $\mathbb{d}$ is the (third-order) tensor of piezoelectric coefficients. For the reversible part of the strain we take

$$\boldsymbol{E}^{\mathrm{rv}} = \mathbb{C}^{-1} : \boldsymbol{T} + \mathbb{d}^{T} \cdot \vec{\mathrm{E}} \tag{9}$$

where $\mathbb{C}$ is the (fourth-order) tensor of elastic moduli ($(\mathbb{d}^{T})_{ijk} = (\mathbb{d})_{kij}$).

The phenomenon of piezoelectricity is connected to a pronounced crystallographic anisotropy of the corresponding material. In particular, its unit cell must not possess a center of symmetry and may be tetragonal, orthorhombic or rhombohedral. However, since we consider a polycrystalline ferroelectric in the sense of a macroscopic approach, a transversely isotropic description is appropriate (cf Chen, 1980; Hwang et al., 1995; Michelitsch and Kreher, 1996). The axis of the transversal isotropy will essentially coincide with the direction of the remanent polarization and the extent of anisotropy depends on the magnitude of the remanent polarization. Furthermore, the remanent strain may have some influence. Thus the state of macroscopic anisotropy results from the loading history and consequently the tensors $\mathbb{d}$, ϵ and $\mathbb{C}$ are functions of the internal variables in general.

In view of the above discussion, we may, for example, take the tensor of dielectric permittivities ϵ to be a function of the remanent polarization $\vec{\mathrm{P}}^{\mathrm{in}}$ in the form

$$\epsilon(\vec{\mathrm{P}}^{\mathrm{in}}) = \epsilon \boldsymbol{I} + \frac{\|\vec{\mathrm{P}}^{\mathrm{in}}\|}{\mathrm{P}_{\mathrm{sat}}} (\epsilon_{\parallel}\, \vec{\mathrm{e}}_{\mathrm{P}^{\mathrm{in}}} \otimes \vec{\mathrm{e}}_{\mathrm{P}^{\mathrm{in}}} + \epsilon_{\perp} (\boldsymbol{I} - \vec{\mathrm{e}}_{\mathrm{P}^{\mathrm{in}}} \otimes \vec{\mathrm{e}}_{\mathrm{P}^{\mathrm{in}}})). \tag{10}$$

The dielectric constant ϵ characterizes the isotropic unpoled state ($\vec{\mathrm{P}}^{\mathrm{in}} = \vec{0}$). For $\vec{\mathrm{P}}^{\mathrm{in}} \neq \vec{0}$, $\epsilon_{\parallel}$ and $\epsilon_{\perp}$

describe the deviation of the dielectricities from the unpoled state in the direction of the poling and perpendicular to it, respectively, yielding a transversally isotropic tensor of dielectric permittivities. However, in order to keep the model as simple as possible, we may neglect the influence of the loading history on $\in$, i.e. $\in_{\parallel}, \in_{\perp} \ll \in$, and assume

$$\in = \in \boldsymbol{I}. \tag{11}$$

In completely analogous manner we may proceed for the transversally isotropic elasticity tensor. But again, we neglect the polarization induced anisotropy and simply use the isotropic elasticity tensor

$$\mathbb{C} = 2\mu\left(\mathbb{I} + \frac{v}{1-2v}\boldsymbol{I}\otimes\boldsymbol{I}\right) \tag{12}$$

where μ and v are the shear modulus and Poisson ratio, respectively ($\mathbb{I}$: identity tensor of fourth-order). These simplified relations for $\in$ and $\mathbb{C}$ might not in any case be appropriate (but see also Hwang et al., 1995).

Concerning $\mathbb{d}(\vec{\mathrm{P}}^{\mathrm{in}})$, the situation is qualitatively different, since the phenomenon of piezoelectricity instead of just being modified is completely absent if there is no net remanent polarization in a polycrystalline ferroelectric. To be specific, we assume for the part of the reversible polarization caused by the mechanical stress

$$\mathbb{d}(\vec{\mathrm{P}}^{\mathrm{in}}) : \boldsymbol{T} = \frac{\|\vec{\mathrm{P}}^{\mathrm{in}}\|}{\mathrm{P}_{\mathrm{sat}}}\{d_{\parallel}\boldsymbol{T}:(\vec{\mathrm{e}}_{\mathrm{P}^{\mathrm{in}}}\otimes\vec{\mathrm{e}}_{\mathrm{P}^{\mathrm{in}}})\vec{\mathrm{e}}_{\mathrm{P}^{\mathrm{in}}} + d_{\perp}\boldsymbol{T}:(\boldsymbol{I}-\vec{\mathrm{e}}_{\mathrm{P}^{\mathrm{in}}}\otimes\vec{\mathrm{e}}_{\mathrm{P}^{\mathrm{in}}})\vec{\mathrm{e}}_{\mathrm{P}^{\mathrm{in}}} + d_{=}(\boldsymbol{I}-\vec{\mathrm{e}}_{\mathrm{P}^{\mathrm{in}}}\otimes\vec{\mathrm{e}}_{\mathrm{P}^{\mathrm{in}}})\cdot(\boldsymbol{T}\cdot\vec{\mathrm{e}}_{\mathrm{P}^{\mathrm{in}}})\}. \tag{13}$$

Note that the direction and the extent of the piezoelectric effect depend on the loading history via $\vec{\mathrm{e}}_{\mathrm{P}^{\mathrm{in}}}$ and $\|\vec{\mathrm{P}}^{\mathrm{in}}\|$, respectively. It may easily be checked that $\mathbb{d}(\vec{\mathrm{P}}^{\mathrm{in}}) : \boldsymbol{T}$ is invariant under proper rotations about an axis through $\vec{\mathrm{P}}^{\mathrm{in}}$, i.e. $\mathbb{d}(\vec{\mathrm{P}}^{\mathrm{in}})$ possesses transverse isotropy without a center of symmetry. The related expression for $\mathbb{d}^{T}(\vec{\mathrm{P}}^{\mathrm{in}})\cdot\vec{\mathrm{E}}$ reads as

$$\begin{aligned}\mathbb{d}^{T}(\vec{\mathrm{P}}^{\mathrm{in}})\cdot\vec{\mathrm{E}} = \frac{\|\vec{\mathrm{P}}^{\mathrm{in}}\|}{\mathrm{P}_{\mathrm{sat}}}\Bigg\{&d_{\parallel}(\vec{\mathrm{E}}\cdot\vec{\mathrm{e}}_{\mathrm{P}^{\mathrm{in}}})(\vec{\mathrm{e}}_{\mathrm{P}^{\mathrm{in}}}\otimes\vec{\mathrm{e}}_{\mathrm{P}^{\mathrm{in}}}) + d_{\perp}(\vec{\mathrm{E}}\cdot\vec{\mathrm{e}}_{\mathrm{P}^{\mathrm{in}}})(\boldsymbol{I}-\vec{\mathrm{e}}_{\mathrm{P}^{\mathrm{in}}}\otimes\vec{\mathrm{e}}_{\mathrm{P}^{\mathrm{in}}})\\ &+ d_{=}\frac{1}{2}[((\boldsymbol{I}-\vec{\mathrm{e}}_{\mathrm{P}^{\mathrm{in}}}\otimes\vec{\mathrm{e}}_{\mathrm{P}^{\mathrm{in}}})\cdot\vec{\mathrm{E}})\otimes\vec{\mathrm{e}}_{\mathrm{P}^{\mathrm{in}}} + \vec{\mathrm{e}}_{\mathrm{P}^{\mathrm{in}}}\otimes((\boldsymbol{I}-\vec{\mathrm{e}}_{\mathrm{P}^{\mathrm{in}}}\otimes\vec{\mathrm{e}}_{\mathrm{P}^{\mathrm{in}}})\cdot\vec{\mathrm{E}})]\Bigg\}.\end{aligned} \tag{14}$$

The piezoelectric constants $d_{\parallel}$, $d_{\perp}$, and $d_{=}$ correspond to the classical constants d_{33}, d_{31}, and d_{15}, respectively. For $\vec{\mathrm{P}}^{\mathrm{in}} = \vec{0}$, no piezoelectric effect is present in our model.

3.3. One-dimensional formulation of the model

As the crucial part of our model, it remains, to formulate the evolution laws for the internal variables $\vec{\mathrm{P}}^{\mathrm{in}}$ and $\boldsymbol{E}^{\mathrm{f}}$. As mentioned before, experimental data on the macroscopic behavior of ferroelectrics suitable for our purposes are rare. Most of the results are available for uniaxial loadings (cf Cao and Evans, 1993; Schäufele, 1996). For this reason, we restrict ourselves for the remainder of this paper to uniaxial loading conditions in the sense that we consider a uniaxial

stress state and a parallel electric field in a fixed direction, which we choose to be the x_3-direction. In the following, we give the notation for the one-dimensional specialization of our model.

We denote the only non-vanishing components of $\boldsymbol{T}$, $\vec{\mathrm{E}}$, $\vec{\mathrm{P}}$, and $\vec{\mathrm{P}}^{\mathrm{in}}$ by σ, E, P, and P^{in}, respectively. Each of the strain tensors $\boldsymbol{E}$, $\boldsymbol{E}^{\mathrm{in}}$, $\boldsymbol{E}^{\mathrm{P}}$, and $\boldsymbol{E}^{\mathrm{f}}$ possess three non-vanishing components: $\varepsilon = E_{33}$, $E_{11} = E_{22}$; $\varepsilon^{\mathrm{in}} = E^{\mathrm{in}}_{33}$, $E^{\mathrm{in}}_{11} = E^{\mathrm{in}}_{22}$; $\varepsilon^{\mathrm{P}} = E^{\mathrm{P}}_{33}$, $E^{\mathrm{P}}_{11} = E^{\mathrm{P}}_{22}$; $\varepsilon^{\mathrm{f}} = E^{\mathrm{f}}_{33}$, $E^{\mathrm{f}}_{11} = E^{\mathrm{f}}_{22}$, respectively. For the remainder of this paper, we consider only the strains in poling direction and pay no attention to the related transverse strains in x_1- and x_2-direction.

The additive decompositions (4) and (5) of the polarization and the uniaxial strain now read as

$$\mathrm{P} = \mathrm{P}^{\mathrm{rv}} + \mathrm{P}^{\mathrm{in}} \tag{15}$$

$$\varepsilon = \varepsilon^{\mathrm{rv}} + \varepsilon^{\mathrm{in}} \tag{16}$$

respectively. According to eqn (6), P^{in} contributes to $\varepsilon^{\mathrm{in}}$ the part

$$\varepsilon^{\mathrm{P}} = \varepsilon_{\mathrm{sat}} \frac{|\mathrm{P}^{\mathrm{in}}|}{\mathrm{P}_{\mathrm{sat}}} \tag{17}$$

and in view of eqn (7) we get for the ferroelastic part

$$\varepsilon^{\mathrm{f}} = \varepsilon^{\mathrm{in}} - \varepsilon^{\mathrm{P}}. \tag{18}$$

From eqns (8), (9), (11)–(13) one finds that the reversible parts of P and ε are related to the electric field E and the uniaxial stress σ by

$$\mathrm{P}^{\mathrm{rv}} = d \frac{\mathrm{P}^{\mathrm{in}}}{\mathrm{P}_{\mathrm{sat}}} \sigma + \epsilon \mathrm{E} \tag{19}$$

$$\varepsilon^{\mathrm{rv}} = \frac{1}{Y} \sigma + d \frac{\mathrm{P}^{\mathrm{in}}}{\mathrm{P}_{\mathrm{sat}}} \mathrm{E} \tag{20}$$

where $Y = 2\mu(1+\nu) = 1/(\mathbb{C}^{-1})_{3333}$ is Young's modulus and $d = d_{\parallel}$. Note that there is no piezoelectric coupling for $\mathrm{P}^{\mathrm{in}} = 0$.

The above system of equations has to be closed by evolution laws for P^{in} and ε^{f}. It has to be pointed out that the generalization of the one-dimensional evolution laws to three-dimensional ones is not a trivial task. It can be done by replacing the one-dimensional components by appropriately chosen vector and tensor invariants. This work is currently on the way, and we will report about it in the near future.

4. Characteristic phenomena of ferroelectricity

4.1. *On the microscopic interpretation some of macroscopic observations*

From a macroscopic point of view, ferroelectricity may be characterized by three typical phenomena: the dielectric hysteresis, the butterfly hysteresis, and the ferroelastic hysteresis, respectively. As far as we consider it as useful for the motivation of our evolution equations, we recall in this

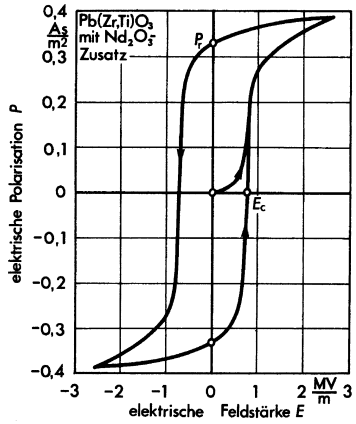

Fig. 2. Dielectric hysteresis measured by H. Thomann, München, for a PZT ceramic (Feldtkeller, 1973).

section some well known microscopic interpretations of these macroscopic phenomena (see the references given in Section 2). We do not at all intend to give a complete survey.

First, we consider purely electric loadings. Figure 2 shows the typical dielectric hysteresis (Feldtkeller, 1973), i.e. the plot of the polarization P over the electric field E. The initially unpoled specimen shows at the beginning nearly linear dielectric behavior. As the electric field approaches the coercitive field, domain switching processes are initiated, and the macroscopic polarization grows rapidly. Upon further increasing the electric field, the alignment of the microscopic polarization of the domains becomes complete, and the rapid growth of the macroscopic polarization saturates. A fully poled state is reached, and after unloading a macroscopic remanent polarization is observed.

We might distinguish three different phases in the material response to the electric loading: a first range of nearly linear reversible behavior for sufficiently small values of the electric field is followed by an intermediate period of domain switching until finally a saturated region of only reversible further polarization changing is reached.

By reversing the electric field beyond a certain threshold, the macroscopic remanent polarization can be reversed (180°-switching). Because of the threshold for the domain switching, a hysteresis loop develops and is completed, if the electric field is increased once more.

A certain similarity to the above discussed non-linear dielectric behavior can be observed, if we consider purely mechanical loadings. This similarity stems from the fact that domain switching processes can be caused either by an electric field or by a mechanical stress. Figure 3 shows the compression part of the ferroelastic hysteresis, i.e. the plot of stress σ vs strain ε for unpoled hard PZT and soft PZT (PIC 141 and PIC 151, respectively. See also Schäufele, 1996 and Cao and Evans, 1993. Note that applying tensile stresses to a ceramic specimen is not a trivial task, cf Fett and Thun, 1997; Fett et al., 1997).

For small stresses, we observe almost linear elastic behavior. If the stress is increased beyond a certain threshold, the coercitive stress, mechanically induced domain switching is initiated (90°-switching). As a consequence, the strain starts to grow much faster. Cao and Evans (1993) measured the Poisson ratio to be equal to 0.5 in this period, thereby supporting the interpretation

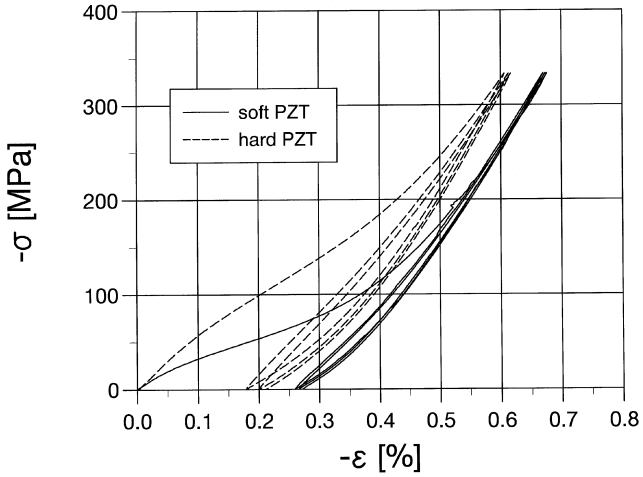

Fig. 3. Uniaxial compression experiment for unpoled hard PZT and soft PZT (PIC 141 and PIC 151, respectively, PI Ceramic, Lederhose (Thüringen), Germany): after the mechanical load is removed, we observe a remanent strain, indicating that mechanically induced domain switching processes have taken place. After domain switching is completed, the mechanical response is approximately elastic.

that the irreversible deformation is caused by domain switching processes. If a fully switched domain structure is reached, the irreversible deformation of the specimen saturates, and we have an approximately elastic response to further loading and unloading. After unloading, we recognize a significant remanent strain.

In switching the domains, a mechanical stress is not able to favor a unique orientation of the domains. An unpoled specimen is left macroscopically unpoled, and a poled specimen looses its macroscopic polarization as shown in Fig. 4 (taken from Schäufele, 1996, see also Cao and Evans, 1993). This phenomenon is called mechanical depolarization.

The probably most typical phenomenon of ferroelectricity is the butterfly hysteresis, i.e. the plot of the strain ε over the electric field E. It demonstrates the electro-mechanical coupling in the form of the strain resulting from domain switching and piezoelectricity under the action of an electric field. Figure 5 shows a typical result for an initially unpoled specimen (Chen and Tucker, 1981).

It is interesting to note that as long as the electric field remains below the coercitive field, no change of the strain is induced. Once the threshold given by the coercitive field is passed, domain switching processes are initiated, which give rise for an irreversible deformation of the specimen. Furthermore, a macroscopic polarization occurs which in turn causes reversible piezoelectric strains. As the domain switching saturates, the increase of the deformation slows down, and upon unloading we observe some reversible piezoelectric recovery of the deformation leaving a significant remanent strain.

By reversing the electric field, eventually domain switching is started again, causing at the beginning a rapid reduction of the macroscopic remanent strain and polarization, respectively. Later on however, the domain structure is oriented more and more in the new direction of the electric field, and remanent strain and macroscopic polarization grow once more. Finally a second fully poled state with piezoelectric behavior and the same maximum remanent strain as before is reached.

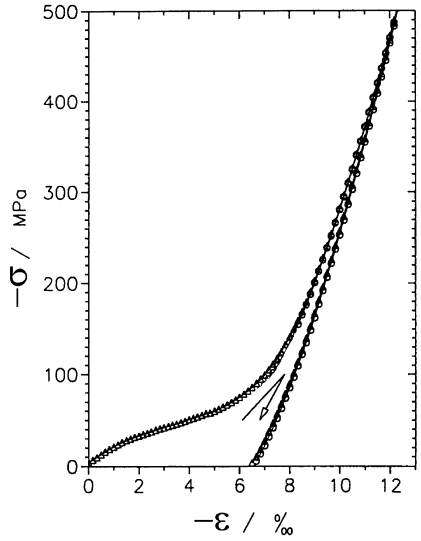

Fig. 4. Mechanical depolarization: mechanical stress over the change in polarization according to Schäufele (1996): under a compressive stress applied parallel to the direction of poling, the polarization is lost gradually as the stress is increased beyond the coercitive stress.

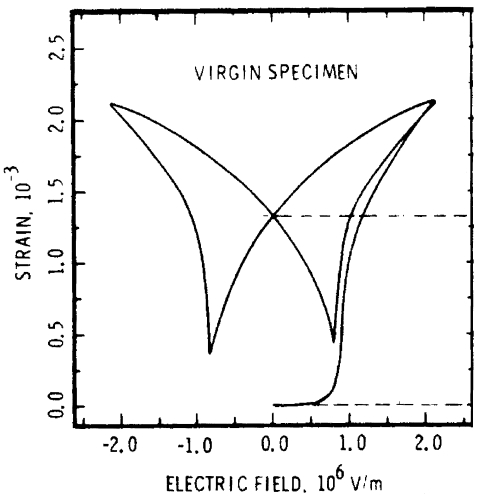

Fig. 5. Butterfly hysteresis: strain ε vs electric field E (Chen and Tucker, 1981). As long as the specimen remains unpoled, no strain can be induced electrically. After unloading, we recognize a remanent strain of 0.13%. During the reversal of the electric field, sharp kinks appear at values of almost zero strain. They indicate the intermediate state of nearly unpoled domain structure between the two fully poled states oriented in the old and the new direction of electric field, respectively.

4.2. Remark on the evolution laws for the internal variables

In the remainder of this paper, we want to motivate evolution laws for the internal variables $\mathbf{P}^{in}$ and ε^{f}. As a guideline we have to find a compromise between simplicity and sophistication. Of course, the model has to catch all the macroscopic phenomena of ferroelectricity we consider essential for computing the stress and other fields as the basis of a reliability analysis. On the other hand, our model has to be as simple as possible in order to keep the computational effort in realistic limits, if it is implemented in an FE-code.

Merely in order to be able to present our model step by step we distinguish in this paper between two levels for the electro-mechanical loading. Restricted electro-mechanical loading means loadings with arbitrary electric fields, but with the mechanical stresses being weak enough, such that no mechanically induced changes of the remanent polarization and the remanent strain are possible. In particular, no mechanical depolarization is possible then, and we have linear elastic mechanical behavior without ferroelastic hysteresis: $\varepsilon^{in} = \varepsilon^{P}$. Rather, the occurrence of electro-mechanical coupling is restricted to linear piezoelectric phenomena. In the case of unrestricted electro-mechanical loading no restriction is made on the magnitude of the loading.

5. Restricted electro-mechanical loading

Each of the internal variables will be subjected to two loading conditions with different physical background. For the sake of simplicity, we will restrict ourselves to a rate independent and bilinear approximation. A more sophisticated representation is possible at the cost of additional internal variables, i.e. additional evolution equations and material parameters. To some extent, we can utilize well-known concepts of incremental plasticity (cf Bassiouny et al., 1988; Bassiouny and Maugin, 1989).

5.1. Dielectric behavior

In order to exemplify our concepts by means of a special case we consider for the moment the purely dielectric behavior, i.e. the relation between P and E without superposed mechanical stress.

In the set of values of E, we postulate the existence of a region of reversible behavior, such that sufficiently small changes of the electric field cause no change of the remanent polarization. Mathematically, we define this region with the help of the function

$$f^{P}(\mathbf{E}, \mathbf{P}^{in}) = |\mathbf{E} - c^{P}\mathbf{P}^{in}| - \mathrm{E}_{c}, \tag{21}$$

where the coercitive field E_{c} and c^{P} are non-negative material constants. The region of reversible behavior is then defined by $f^{P}(\mathbf{E}, \mathbf{P}^{in}) \leqslant 0$, i.e.

$$\dot{\mathbf{P}}^{in} = 0 \quad \text{for} \quad f^{P}(\mathbf{E}, \mathbf{P}^{in}) < 0 \quad \text{or} \quad \frac{\mathrm{d}}{\mathrm{d}t} f^{P}(\mathbf{E}, \mathbf{P}^{in})\,|_{\dot{\mathbf{P}}^{in}=0} \leqslant 0. \tag{22}$$

In particular, as long as the absolute value of the electric field E is smaller than the coercitive field, no remanent polarization can be induced.

If the condition of reversibility is no longer fulfilled, $\mathbf{P}^{\mathrm{in}}$ is assumed to change in the direction of the acting electric field:

$$\dot{\mathbf{P}}^{\mathrm{in}} = \frac{\dot{\mathbf{E}}}{c^{\mathrm{P}}} \quad \text{for} \quad f^{\mathrm{P}}(\mathbf{E}, \mathbf{P}^{\mathrm{in}}) = 0 \quad \text{and} \quad \frac{\mathrm{d}}{\mathrm{d}t} f^{\mathrm{P}}(\mathbf{E}, \mathbf{P}^{\mathrm{in}}) \,|_{\dot{\mathbf{P}}^{\mathrm{in}} = 0} > 0. \tag{23}$$

Since this evolution equation is homogeneous of degree 1 in first-order derivatives with respect to time, it yields a rate independent evolution for $\mathbf{P}^{\mathrm{in}}$. Furthermore, the consistency condition $\dot{f}^{\mathrm{P}}(\mathbf{E}, \mathbf{P}^{\mathrm{in}}) = 0$ is satisfied.

So far, we could rely on some well known mathematical tools of incremental plasticity. However, there is a fundamental difference between the physical mechanism of dislocation movement resulting in plastic deformation of metals and the domain switching of ferroelectrics: in the fully poled state ($|\mathbf{P}^{\mathrm{in}}| = \mathrm{P}_{\mathrm{sat}}$), no further domain switching and thus no further growth of the remanent polarization is possible. This motivates us to introduce a second criterion indicating the fully poled state with the help of the function

$$h^{\mathrm{P}}(\mathbf{P}^{\mathrm{in}}) = |\mathbf{P}^{\mathrm{in}}| - \mathrm{P}_{\mathrm{sat}} \tag{24}$$

and we demand

$$\dot{\mathbf{P}}^{\mathrm{in}} = 0 \quad \text{for} \quad h^{\mathrm{P}}(\mathbf{P}^{\mathrm{in}}) = 0 \quad \text{and} \quad \frac{\mathrm{d}}{\mathrm{d}t} h^{\mathrm{P}}(\mathbf{P}^{\mathrm{in}}) \,|_{\dot{\mathbf{P}}^{\mathrm{in}} = \dot{\mathbf{E}}/c^{\mathrm{P}}} > 0. \tag{25}$$

This means that even for an increasing absolute value of the electric field the magnitude of the remanent polarization cannot exceed the saturation polarization $\mathrm{P}_{\mathrm{sat}}$.

Two criteria, $f^{\mathrm{P}} \leqslant 0$ and $h^{\mathrm{P}} \leqslant 0$, control the evolution of $\mathbf{P}^{\mathrm{in}}$. In general, these criteria cannot be satisfied at the same time. In our model, the h-criterion has the higher priority, and $f^{\mathrm{P}} > 0$ is possible if case (25) applies. In this case, the consistency condition $\dot{h}^{\mathrm{P}}(\mathbf{P}^{\mathrm{in}}) = 0$ is fulfilled. For a closed mathematical formulation of the evolution law taking into account the different cases, we introduce some definitions. First, let

$$\lfloor x \rceil = \begin{cases} 1, & x \geqslant 0 \\ 0, & x < 0 \end{cases} \tag{26}$$

and

$$\lceil x \rfloor = \begin{cases} 1, & \mathrm{x} > 0 \\ 0, & \mathrm{x} \leqslant 0 \end{cases}. \tag{27}$$

Furthermore, let

$$\overset{*}{f}{}^{\mathrm{P}} = \frac{\mathrm{d}}{\mathrm{d}t} f^{\mathrm{P}} \bigg|_{\dot{\mathbf{P}}^{\mathrm{in}} = 0} \tag{28}$$

and

$$\overset{*}{h}{}^{\mathrm{P}} = \frac{\mathrm{d}}{\mathrm{d}t} h^{\mathrm{P}} \Big|_{\dot{\mathrm{P}}^{\mathrm{in}} = \lfloor f^{\mathrm{P}} \rfloor \lfloor \overset{*}{f}{}^{\mathrm{P}} \rfloor \dot{\mathrm{E}}/c^{\mathrm{P}}}. \tag{29}$$

We then may write

$$\dot{\mathrm{P}}^{\mathrm{in}} = \left(1 - \lceil \lfloor h^{\mathrm{P}} \rfloor \lceil \overset{*}{h}{}^{\mathrm{P}} \rfloor + \lceil f^{\mathrm{P}} \rfloor \right) \lfloor f^{\mathrm{P}} \rfloor \lfloor \overset{*}{f}{}^{\mathrm{P}} \rfloor \frac{\dot{\mathrm{E}}}{c^{\mathrm{P}}}. \tag{30}$$

It may readily be checked that the cases (22), (23), and (25) are covered by this formula. The term $\lceil f^{\mathrm{P}} \rfloor$ expresses the fact that the h-criterion has to be satisfied as long as the f-criterion is violated. The significance of this term will become more obvious as soon as the phenomenon of mechanical depolarization is incorporated into the model.

5.2. The dielectric hysteresis

As an example, we consider the first polarization curve, i.e. vanishing remanent polarization as initial condition and a monotonically increasing electric field. For this case, eqns (15), (19), (22), (23) and (25) yield

$$\mathrm{P}(\mathrm{E}) = \begin{cases} \epsilon \mathrm{E}, & 0 \leqslant \mathrm{E} < \mathrm{E}_{\mathrm{c}} \\ \dfrac{1 + c^{\mathrm{P}} \epsilon}{c^{\mathrm{P}}} \mathrm{E} - \dfrac{\mathrm{E}_{\mathrm{c}}}{c^{\mathrm{P}}}, & \mathrm{E}_{\mathrm{c}} \leqslant \mathrm{E} < \mathrm{E}_{\mathrm{c}} + c^{\mathrm{P}} \mathrm{P}_{\mathrm{sat}}. \\ \epsilon \mathrm{E} + \mathrm{P}_{\mathrm{sat}}, & \mathrm{E}_{\mathrm{c}} + c^{\mathrm{P}} \mathrm{P}_{\mathrm{sat}} \leqslant \mathrm{E} \end{cases} \tag{31}$$

Obviously, the first polarization curve is represented by three straight lines if P is plotted over E. Each part corresponds to a different case. In the first case, $f^{\mathrm{P}} < 0$ and $h^{\mathrm{P}} < 0$, then $f^{\mathrm{P}} = 0$ and $h^{\mathrm{P}} < 0$, and finally $f^{\mathrm{P}} > 0$ and $h^{\mathrm{P}} = 0$. Equation (31) realizes, strictly speaking, a three linear approximation of the first polarization curve. However, since both the starting and the saturated slopes are given by the dielectric constant ε because of the isotropy assumption (11), we may use the term 'bilinear approximation', which is common in plasticity. The constant c^{P} effects the slope of the intermediate part of the P–E-graph, during which the remanent polarization grows from 0–$\mathrm{P}_{\mathrm{sat}}$, i.e. the poling takes place.

If now in a second step, the electric field is reversed by decreasing it monotonically from above $\mathrm{E}_{\mathrm{c}} + c^{\mathrm{P}} \mathrm{P}_{\mathrm{sat}}$ to a value below $-\mathrm{E}_{\mathrm{c}} - c^{\mathrm{P}} \mathrm{P}_{\mathrm{sat}}$, we get

$$\mathrm{P}(\mathrm{E}) = \begin{cases} \epsilon \mathrm{E} + \mathrm{P}_{\mathrm{sat}}, & -\mathrm{E}_{\mathrm{c}} + c^{\mathrm{P}} \mathrm{P}_{\mathrm{sat}} < \mathrm{E} \\ \dfrac{1 + c^{\mathrm{P}} \epsilon}{c^{\mathrm{P}}} \mathrm{E} + \dfrac{\mathrm{E}_{\mathrm{c}}}{c^{\mathrm{P}}}, & -\mathrm{E}_{\mathrm{c}} - c^{\mathrm{P}} \mathrm{P}_{\mathrm{sat}} < \mathrm{E} \leqslant -\mathrm{E}_{\mathrm{c}} + c^{\mathrm{P}} \mathrm{P}_{\mathrm{sat}}. \\ \epsilon \mathrm{E} - \mathrm{P}_{\mathrm{sat}}, & \mathrm{E} \leqslant -\mathrm{E}_{\mathrm{c}} - c^{\mathrm{P}} \mathrm{P}_{\mathrm{sat}} \end{cases} \tag{32}$$

Again, we observe three different parts for the polarization plotted over the electric field. In particular, the second part represents the process of 180° polarization switching from $\mathrm{P}^{\mathrm{in}} = \mathrm{P}_{\mathrm{sat}}$–$\mathrm{P}^{\mathrm{in}} = -\mathrm{P}_{\mathrm{sat}}$ induced by reversing the electric field. The dielectric hysteresis is closed, if the electric

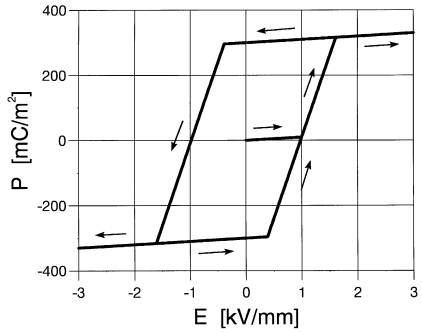

Fig. 6. Bilinear approximation of the dielectric hysteresis (polarization P plotted vs the electric field E): the slopes of the starting and the saturated parts are the same ($=\in$). The slope of the intermediate phase of irreversible polarization changing (polarization switching) depends additionally on c^{P}. The first onset of polarization switching occurs at $E = E_c$. After unloading ($E = 0$), $|P|$ assumes the value P_{sat}.

field is reversed once more (see Fig. 6). The values of the material constants chosen for the calculations with the model of this paper are given in Table 1.

As a first coupling phenomenon we consider the dielectric hysteresis for the case of a superposed static stress. In the present stage (restricted electro-mechanical loading), we restrict ourselves to stresses low enough such that no mechanically induced polarization switching occurs. According to eqn (19), the reversible polarization P^{rv} includes then the mechanical contribution $d(P^{in}/P_{sat})\sigma$. Figure 7 clearly demonstrates the resulting direct piezoelectric effect: the reversible and thus the total polarization is reduced under compressive and enlarged under tensile stresses, respectively. In the fully poled state ($|P^{in}| = P_{sat}$), this effect amounts to σd.

5.3. The butterfly hysteresis

Equation (17) relates the magnitude of the remanent polarization and the induced remanent strain as being proportional to each other such that $\varepsilon^{P} = \varepsilon_{sat}$ for $|P^{in}| = P_{sat}$. A further contribution to the butterfly hysteresis stems from the piezoelectric coupling term in eqn (20): the inverse piezoelectric effect yields the reversible part of the electrically induced strain which is proportional to the electric field for given P^{in}.

Figure 8 shows the butterfly hysteresis starting from an unpoled state in absence of a superposed mechanical stress. The loading history starts from $E = 0$, and ε^{P} and ε^{rv} remain at zero value as

Table 1
Values of the material constants chosen for the calculations with the model of this paper

E_c	kV/mm	1.0	m	MPa	50.0
P_{sat}	mC/m^2	300	σ_c	MPa	50.0
d	mm/kV	0.001	ε_{sat}	%	0.2
$\in$	mC/kVm	0.01	Y	MPa	100
c^{P}	kVm/mC	2.0	c^{f}	MPa	5.3

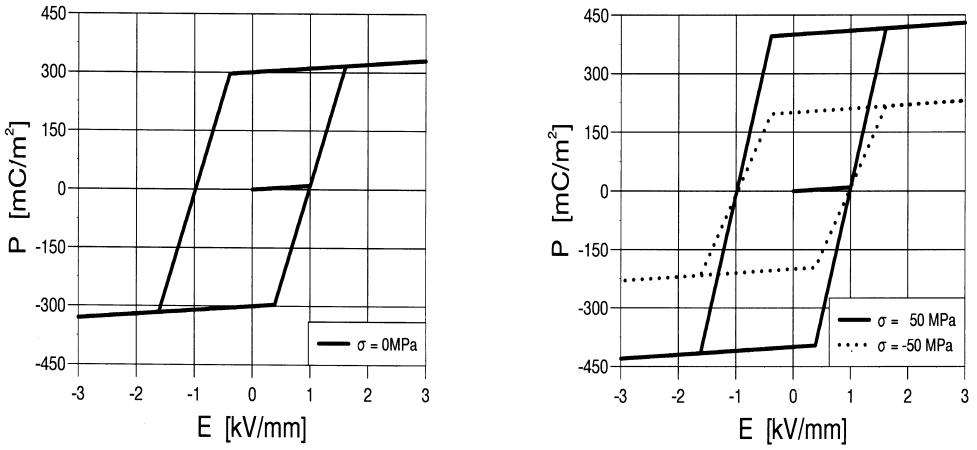

Fig. 7. Dielectric hysteresis under superposed static stress σ: a tensile stress yields a larger polarization, while the polarization is reduced under compression (direct piezoelectric effect). In the fully poled state, the difference is σd.

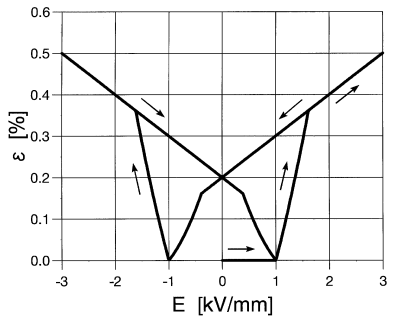

Fig. 8. Butterfly hysteresis (strain ε plotted over the electric field E) : after poling, the strain $\varepsilon-\varepsilon_{sat}$ and the electric field are related linearly to each other with the piezoelectric constant d as the factor of proportionality. However, if the changes of the electric field exceed certain limits, hysteresis effects occur.

long as $E < E_c$, since $P^{in} = 0$ then. In the period $E_c \leqslant E < E_c + c^P P_{sat}$, the remanent polarization grows from zero to the saturation polarization, and ε changes quadratically with respect to the electric field. At $E = E_c + c^P P_{sat}$ we observe a second kink since the h^P-criterion is satisfied from then on ($P^{in} = P_{sat}$). Only the value of ε^{rv} increases further and the slope is equal to the piezoelectric constant d.

After unloading, we find a remanent strain equal to ε_{sat}. In this poled state, we have linear piezoelectric behavior relative to the saturation strain ε_{sat} with d as piezoelectric constant, as long as the electric field is not reversed too far. However, for $E \leqslant -E_c + c^P P_{sat}$, the remanent polarization becomes gradually reversed. As a consequence, ε starts to decrease rapidly, and for $P^{in} = 0$, ε is equal to zero, but it grows again for $P^{in} < 0$. At $E = -E_c - c^P P_{sat}$ the remanent polarization is completely switched ($P^{in} = -P_{sat}$), and we have a second range of reversible piezoelectric changing.

Next we consider the case of a superposed static stress of moderate amount. According to eqn

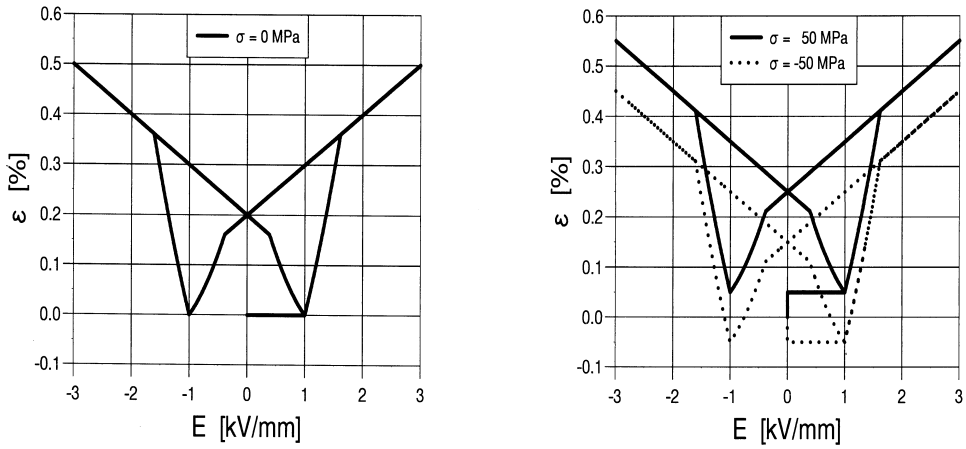

Fig. 9. Butterfly hysteresis under superposed static stress σ: a tensile stress results in an additional positive strain, while compression yields a negative additive contribution.

(20), we have then an additional constant contribution σ/Y to the strain (cf Fig. 9). This additive part is positive for tensile and negative for compressive stresses, respectively.

6. Unrestricted electro-mechanical loading

From now on, we dismiss the restrictions imposed on the mechanical stress in the last section. The model will be extended such that the additional phenomena related to stress induced domain switching can be represented. To begin with, we consider purely mechanical loading, i.e. the ferroelastic hysteresis.

6.1. Ferroelastic behavior

In absence of an electric field, the macroscopic remanent polarization vanishes ($\mathrm{P}^{\mathrm{in}} = 0$), and thus by eqn (17), the remanent strain induced by the remanent polarization ε^{P} is equal to zero as well. Then, it follows from eqn (18) that only mechanically induced, i.e. ferroelastic, remanent strains occur: $\varepsilon^{\mathrm{in}} = \varepsilon^{\mathrm{f}}$.

From the uniaxial compression experiment in Fig. 3, we may identify three different parts. A first range of reversible behavior is followed by an intermediate period of mechanically induced domain switching until a fully switched state with linear reversible behavior and the remanent saturation strain is reached. This interpretation of the experimental result motivates us to model ferroelastic behavior by complete analogy to the dielectric part of the model. Therefore, we confine ourselves to give a brief sketch of the model obtained this way.

With the help of the function

$$f^{\mathrm{f}}(\sigma, \varepsilon^{\mathrm{f}}) = |\sigma - c^{\mathrm{f}}\varepsilon^{\mathrm{f}}| - \sigma_{\mathrm{c}} \tag{33}$$

we define a range of reversible ('elastic') mechanical behavior such that

$$\dot{\varepsilon}^{\mathrm{f}} = 0 \quad \text{for} \quad f^{\mathrm{f}}(\sigma, \varepsilon^{\mathrm{f}}) < 0 \quad \text{or} \quad \frac{\mathrm{d}}{\mathrm{d}t} f^{\mathrm{f}}(\sigma, \varepsilon^{\mathrm{f}})|_{\dot{\varepsilon}^{\mathrm{f}}=0} \leqslant 0. \tag{34}$$

The coercitive stress σ_{c} and c^{f} are non-negative material constants.

If the above condition of reversibility is no longer satisfied, the ferroelastic remanent strain is assumed to change into the direction of the applied stress according to

$$\dot{\varepsilon}^{\mathrm{f}} = \frac{\dot{\sigma}}{c^{\mathrm{f}}} \quad \text{for} \quad f^{\mathrm{f}}(\sigma, \varepsilon^{\mathrm{f}}) = 0 \quad \text{and} \quad \frac{\mathrm{d}}{\mathrm{d}t} f^{\mathrm{f}}(\sigma, \varepsilon^{\mathrm{f}})\,|_{\dot{\varepsilon}=0} > 0. \tag{35}$$

This is a rate-independent evolution equation satisfying the consistency condition $\dot{f}^{\mathrm{f}}(\sigma, \varepsilon^{\mathrm{f}}) = 0$. As a consequence, the tangent modulus on the ε–σ-graph associated to mechanically induced domain switching depends on the constant c^{f} (besides depending on Young's modulus Y).

Finally, we introduce the function

$$h^{\mathrm{f}}(\varepsilon^{\mathrm{f}}) = |\varepsilon^{\mathrm{f}}| - \varepsilon_{\mathrm{sat}} \tag{36}$$

for a criterion indicating the saturation strain $\varepsilon_{\mathrm{sat}}$ belonging to a fully switched domain structure:

$$\dot{\varepsilon}^{\mathrm{f}} = 0 \quad \text{for} \quad h^{\mathrm{f}}(\varepsilon^{\mathrm{f}}) = 0 \quad \text{and} \quad \frac{\mathrm{d}}{\mathrm{d}t} h^{\mathrm{f}}(\varepsilon^{\mathrm{f}})\,|_{\dot{\varepsilon}^{\mathrm{f}}=\dot{\sigma}/c^{\mathrm{f}}} > 0. \tag{37}$$

With the definitions

$$\overset{*}{f}{}^{\mathrm{f}} = \frac{\mathrm{d}}{\mathrm{d}t} f^{\mathrm{f}}\bigg|_{\dot{\varepsilon}^{\mathrm{f}}=0} \tag{38}$$

and

$$\overset{*}{h}{}^{\mathrm{f}} = \frac{\mathrm{d}}{\mathrm{d}t} h^{\mathrm{f}}\bigg|_{\dot{\varepsilon}^{\mathrm{f}}=\lfloor f^{\mathrm{f}}\rceil \lfloor \overset{*}{f}{}^{\mathrm{f}}\rceil \dot{\sigma}/c^{\mathrm{f}}} \tag{39}$$

we may write by analogy to eqn (30)

$$\dot{\varepsilon}^{\mathrm{f}} = \left(1 - \left\lceil \lfloor h^{\mathrm{f}}\rceil \lceil \overset{*}{h}{}^{\mathrm{f}}\rfloor + \lceil f^{\mathrm{f}}\rfloor \right\rfloor\right) \lfloor f^{\mathrm{f}}\rceil \lfloor \overset{*}{f}{}^{\mathrm{f}}\rceil \frac{\dot{\sigma}}{c^{\mathrm{f}}}. \tag{40}$$

Figure 10 shows the response of the mechanical part of the model to cyclic stress controlled loading, i.e. eqns (16), (18), (20) and (33)–(37). Obviously, our model implies an extrapolation of the experimental result in Fig. 3, since the response to tensile and compressive loadings is represented symmetrically with respect to the state $(\varepsilon, \sigma) = (0, 0)$ (for an experimental investigation of this topic see Fett et al., 1997). We recognize a bilinear approximation with three different ranges in the plot of the stress σ over the strain ε. A first range of reversible response, an intermediate phase, during which the ferroelastic remanent strain develops, and a part where the remanent strain has reached its saturation value. Because of the isotropy assumption (12), both the slopes of the first and the third part of the mechanical response are equal to Y.

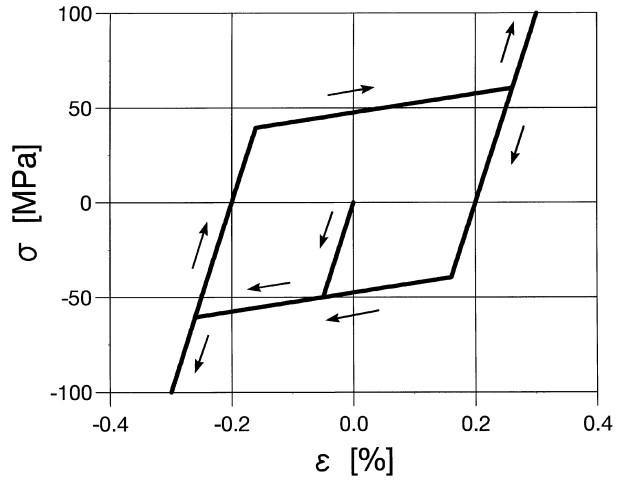

Fig. 10. Ferroelastic hysteresis (stress σ vs strain ε): the model response is symmetrical with respect to the origin. The slopes of the starting and the saturated parts are the same ($=Y$). The tangent modulus of the intermediate phase of irreversible deformation depends additionally on c^{r}. The first onset of remanent deformation occurs at $\sigma=\sigma_{\mathrm{c}}$. After unloading ($\sigma=0$), $|\varepsilon|$ assumes the value $\varepsilon_{\mathrm{sat}}$.

6.2. History dependent saturation polarization

In the framework of our model, we interpret the phenomenon of mechanical depolarization such, that the maximum absolute value of the macroscopic remanent polarization depends on the loading history. In this sense, we assume this saturation value in the h^{P}-criterion no longer to be a constant, but rather to be a material function, i.e.

$$h^{\mathrm{P}}=|\mathrm{P}^{\mathrm{in}}|-\hat{\mathrm{P}}_{\mathrm{sat}}(\sigma,\mathrm{E},\mathrm{P}^{\mathrm{in}}). \tag{41}$$

In particular, it is required that

$$\hat{\mathrm{P}}_{\mathrm{sat}}(\sigma,0,\mathrm{P}^{\mathrm{in}})=\mathrm{P}_{\mathrm{sat}}\quad\text{for }\sigma\geqslant-\sigma_{\mathrm{c}}, \tag{42}$$

where the constant $\mathrm{P}_{\mathrm{sat}}$ is the saturation polarization introduced in the previous sections. This condition implies that only compressive stresses of sufficient magnitude are able to reduce the maximum absolute value of the macroscopic remanent polarization, i.e. to cause mechanical depolarization.

In order to justify these assumptions a posteriori, we now choose as a simple example

$$\hat{\mathrm{P}}_{\mathrm{sat}}(\sigma)=\mathrm{P}_{\mathrm{sat}}\,\mathrm{e}^{-\langle-\sigma-\sigma_{\mathrm{c}}\rangle/m}. \tag{43}$$

In this equation, the MacCauley bracket $\langle\cdot\rangle$ has the property $\langle x\rangle=0$ for $x\leqslant 0$ and $\langle x\rangle=x$ for $x\geqslant 0$. In the above special case, $\hat{\mathrm{P}}_{\mathrm{sat}}$ is independent of the electric field and the remanent polarization. Obviously, condition (42) is met. The positive constant m governs the progress of the mechanical depolarization. If the influence of the electric field on the mechanical depolarization behavior is to be represented, a more general form can be chosen for $\hat{\mathrm{P}}_{\mathrm{sat}}$.

In general, the rate of P^{in} no longer simply vanishes, once the h^{P}-criterion is fulfilled. Rather,

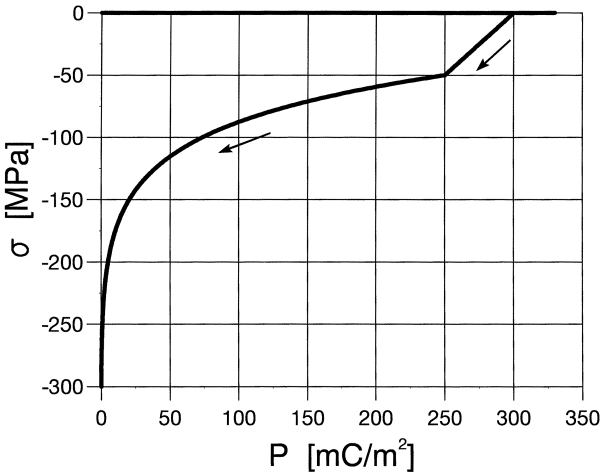

Fig. 11. Mechanical depolarization (polarization P vs stress σ). The horizontal line at $\sigma = 0$ corresponds to the poling process. For stresses $0 \geqslant \sigma \geqslant -\sigma_c$, we observe linear piezoelectric changes of the polarization [eqn (15)]. Once the threshold $-\sigma_c$ is overcome, the polarization is reduced essentially due to the exponentially decreasing remanent polarization P^{in} [eqn (43)]. The reduction of P^{in} causes the piezoelectricity, i.e. P^{rv}, to vanish leaving a material without electro-mechanical coupling.

the consistency condition $\dot{h}^{\mathrm{P}} = 0$ yields an evolution proportional to the stress rate and the evolution law (30) is extended by an additional term:

$$\dot{\mathrm{P}}^{\mathrm{in}} = \left(1 - \left\lceil \lfloor h^{\mathrm{P}} \rceil \lceil \overset{*}{h}{}^{\mathrm{P}} \rfloor + \lceil f^{\mathrm{P}} \rfloor \right\rfloor\right) \lfloor f^{\mathrm{P}} \rceil \lfloor \overset{*}{f}{}^{\mathrm{P}} \rceil \frac{\dot{\mathrm{E}}}{c^{\mathrm{P}}} + \left\lceil \lfloor h^{\mathrm{P}} \rceil \lceil \overset{*}{h}{}^{\mathrm{P}} \rfloor + \lceil f^{\mathrm{P}} \rfloor \right\rfloor \operatorname{sgn}(\mathrm{P}^{\mathrm{in}}) \frac{\mathrm{d}}{\mathrm{d}\sigma} \hat{\mathrm{P}}_{\mathrm{sat}}(\sigma) \dot{\sigma}. \tag{44}$$

For the example (43), we find

$$\frac{\mathrm{d}}{\mathrm{d}\sigma} \hat{\mathrm{P}}_{\mathrm{sat}}(\sigma) = \frac{1}{m} \hat{\mathrm{P}}_{\mathrm{sat}}(\sigma) \mathrm{H}(-\sigma - \sigma_c) \tag{45}$$

where $\mathrm{H}(\cdot)$ is the Heaviside function.

As long as neither the f-criterion nor the h-criterion are satisfied, P^{in} is constant. Once the f-criterion is met, P^{in} evolves according to the first term in eqn (44) proportionally to $\dot{\mathrm{E}}$. However, as soon as the h-criterion is fulfilled, the second term in eqn (44) is active. From eqn (45) it can be seen that this term contains a loading condition: only for compressive stresses below the coercitive stress, i.e. $\mathrm{H}(-\sigma - \sigma_c) = 1$, P^{in} can change proportionally to the stress rate.

For an initially poled and unstressed ferroelectric ($\mathrm{P}(t_0) = \mathrm{P}^{\mathrm{in}}(t_0) = \pm \mathrm{P}_{\mathrm{sat}}$), we find from eqns (15), (41), (43), (44), and (19)

$$\mathrm{P} = \mathrm{P}^{\mathrm{in}} + \mathrm{P}^{\mathrm{rv}} = \pm \mathrm{P}_{\mathrm{sat}} \, \mathrm{e}^{-\langle -\sigma - \sigma_c \rangle / m} \left(1 + \frac{\mathrm{d}}{\mathrm{P}_{\mathrm{sat}}} \sigma\right) \tag{46}$$

for the mechanical depolarization, i.e. the plot of the polarization over a monotonically increasing compressive stress ($\mathrm{E}(t) = 0$, see Fig. 11).

In view of eqns (17) and (44), we see that in general the remanent strain ε^{P} induced by the

remanent polarization P^{in} does not depend on the history of E alone. Rather, it may also be changed by a mechanical stress σ : a mechanical depolarization, i.e. a mechanically caused reduction of P^{in}, yields a corresponding reduction of the related remanent strain ε^{P}, since it is a function of the remanent polarization.

6.3. A compatibility condition for the magnitude of the remanent strain

For an arbitrary electro-mechanical loading history, we have to take care that the magnitude of the macroscopic remanent strain never exceeds its saturation value $\varepsilon_{\mathrm{sat}}$. In the present stage of the model, this is guaranteed for purely electric or purely mechanical loadings only. According to eqns (17) and (18), both of the independent internal variables P^{in} and ε^{f} contribute to the remanent strain :

$$\varepsilon^{\mathrm{in}} = \varepsilon^{\mathrm{f}} + \varepsilon_{\mathrm{sat}} \frac{|\mathrm{P}^{\mathrm{in}}|}{\mathrm{P}_{\mathrm{sat}}}. \tag{47}$$

Consequently, $|\varepsilon^{\mathrm{in}}|$ might assume values up to $2\varepsilon_{\mathrm{sat}}$ under combined electro-mechanical loadings according to the actual version of the model.

In our interpretation, the reservoir for the purely ferroelastic remanent strain ε^{f} is limited by the amount of strain, which is associated to the macroscopic remanent polarization, i.e. ε^{P}. In this sense, we replace in the h^{f}-criterion (36) the saturation strain by the difference $\varepsilon_{\mathrm{sat}} - |\varepsilon^{\mathrm{P}}|$ in order to overcome the above mentioned shortcoming yielding

$$h^{\mathrm{f}}(\varepsilon^{\mathrm{f}}, \mathrm{P}^{\mathrm{in}}) = |\varepsilon^{\mathrm{f}}| - \varepsilon_{\mathrm{sat}} \left(1 - \frac{|\mathrm{P}^{\mathrm{in}}|}{\mathrm{P}_{\mathrm{sat}}} \right). \tag{48}$$

It may be easily seen from eqns (47) and (48) that ε^{f} and ε^{P} now are compatible in the sense $|\varepsilon^{\mathrm{in}}(t)| \leqslant \varepsilon_{\mathrm{sat}}$.

Now, the consistency condition $\dot{h}^{\mathrm{f}} = 0$ yields

$$\dot{\varepsilon}^{\mathrm{f}} = \left(1 - \left\lceil \lfloor h^{\mathrm{f}} \rceil \lceil \overset{*}{h}{}^{\mathrm{f}} \rfloor + \lceil f^{\mathrm{f}} \rfloor \right\rfloor \right) \lfloor f^{\mathrm{f}} \rceil \lfloor \overset{*}{f}{}^{\mathrm{f}} \rceil \frac{\dot{\sigma}}{c^{\mathrm{f}}} - \left\lceil \lfloor h^{\mathrm{f}} \rceil \lceil \overset{*}{h}{}^{\mathrm{f}} \rfloor + \lceil f^{\mathrm{f}} \rfloor \right\rfloor \frac{\varepsilon_{\mathrm{sat}}}{\mathrm{P}_{\mathrm{sat}}} \operatorname{sgn}(\mathrm{P}^{\mathrm{in}}) \operatorname{sgn}(\varepsilon^{\mathrm{f}}) \dot{\mathrm{P}}^{\mathrm{in}} \tag{49}$$

where $\dot{\mathrm{P}}^{\mathrm{in}}$ has to be replaced according to eqn (44).

In view of eqns (49) and (44), we recognize that the ferroelastic remanent strain ε^{f} depends both on the histories of σ and E. From eqns (17), (44), and (49) we conclude that the remanent strain $\varepsilon^{\mathrm{in}}$ depends in a complicated non-linearly coupled manner on the histories of the stress and the electric field.

7. Discussion and conclusion

In closing, we want to discuss the model response to a more complex electro-mechanical loading path. The loading history depicted in Fig. 12(a) is divided in five steps. The electric field is raised to $3\mathrm{E}_{\mathrm{c}}$ in the first step (a) and kept constant in the second step, during which a strong compressive stress is applied (B). In the third step, the mechanical stress is constant and the electric field is

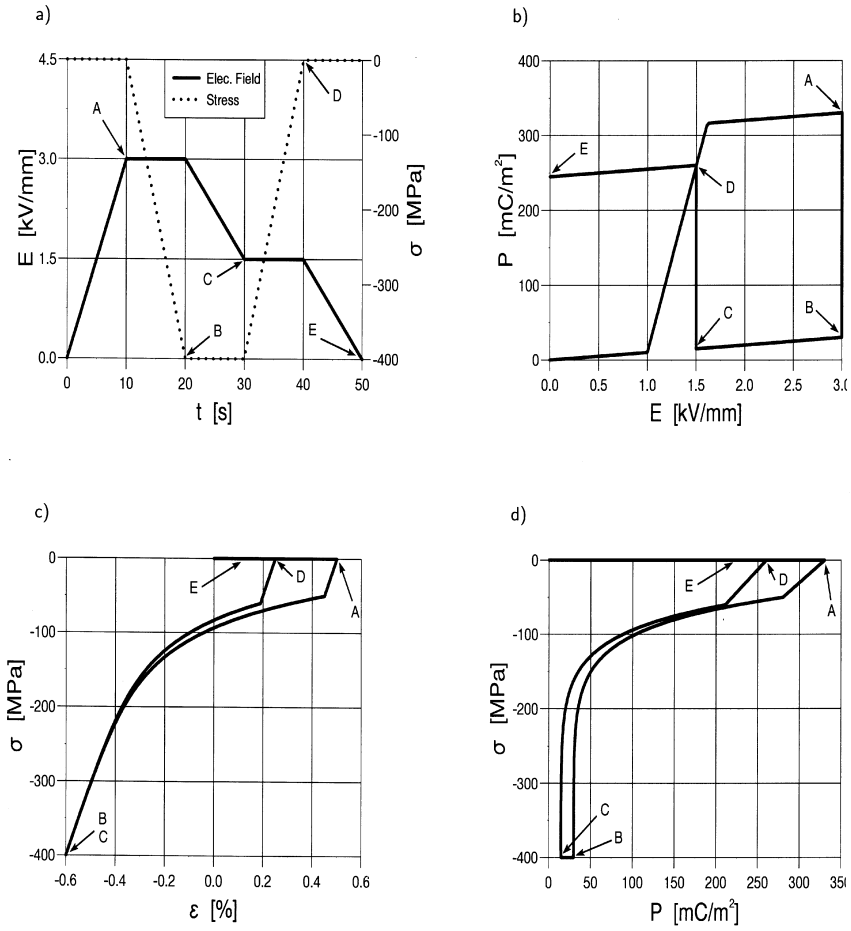

Fig. 12. Model response to a more complex loading path (the capital letters in Figs (b)–(d) indicate the end of the corresponding load step in Fig. (a)) : (a) electro-mechanical loading history E(t), $\sigma(t)$; (b) polarization P vs electric field E ; (c) stress σ vs strain ε ; (d) stress σ vs polarization P.

reduced to 1.5 E_c (C). It remains at this value in the fourth step, while the mechanical stress is completely removed (D). Finally, the electric field is reduced to zero in the fifth step (E).

In the first step (A), we observe a poling process (cf Fig. 12(b)), i.e. a rapid increase of the polarization once the coercitive field is overcome, until the remanent polarization reaches its saturation value and further polarization changes are reversible. The reversible and irreversible straining associated to the poling process can be seen in Fig. 12(c).

In the second step (B), mechanical depolarization takes place. From Fig. 12(d) we see that the polarization is reduced under the action of a strong compressive load. First, we observe linear piezoelectric changing but for stresses below the coercitive stress, an exponential decrease of the remanent polarization starts. As can be seen in Fig. 12(b), the remaining polarization is merely the linear dielectric contribution associated to the electric field by the dielectric constant. Figure

12(c) shows the deformation resulting from changing the remanent strain from $+\varepsilon_{sat}$ to $-\varepsilon_{sat}$ and the elastic part σ/Y.

The third step (C) leads to a linear dielectric reduction of the polarization (cf Fig. 12(b) and (c)). In the fourth step (D), the mechanical stress is removed. However, the electric field is still above the coercitive field, and thus the remanent polarization recovers until it reaches the corresponding value of the first polarization curve in Fig. 12(b). Furthermore, we have an associated recovery of the remanent strain (Fig. 12(c)). Finally, upon removing in step five (E) the electric field, the polarization and the strain are reduced to their current remanent values.

The further development of the model is currently on the way. First, it has become clear from the above discussion that the mechanical depolarization behavior of the model is independent of the applied electric field (in this respect cf the experimental results of Schäufele, 1996 and Schäufele and Härdtl, 1996). This is caused by the simplifying eqn (43), which can be replaced by a more sophisticated choice by assuming the coercitive stress to be a material function (cf Kamlah et al., 1997). Second, the evolution laws (44) and (49) have to be generalized to a three-dimensional form. For this purpose, vector and tensor invariants are introduced to replace the uniaxial quantities. After this job has been done, the model can be implemented in a finite element code by means of an appropriate integration algorithm.

After submitting the first version of this paper, the publication Bertram (1982) came to our notice. The mechanical behavior of shape memory alloys is described on the basis of loading conditions with analogous meaning as our *f*- and *h*-criteria. Even though it seems to us that the work is kind of incomplete with respect to the formulation of the saturation criterion (*h*-criterion), it is interesting to note the similarity in the motivation for a phenomenological approach.

Acknowledgements

We thank Ulrich Böhle for his contribution to this work. Support by the Deutsche Forschungsgemeinschaft, Bonn, is gratefully acknowledged.

References

Bassiouny, E., Ghaleb, A.F., Maugin, G.A., 1988. Thermomechanical formulation for coupled electromechanical hysteresis effects—I. Basic equations, II. Poling of ceramics. Int. J. Engng Sci. 26, 1279–1306.

Bassiouny, E., Maugin, G.A., 1989. Thermomechanical formulation for coupled electromechanical hysteresis effects—III. Parameter identification, IV. Combined electromechanical loading. Int. J. Engng Sci. 27, 975–1000.

Bertram, A., 1982. Thermo-mechanical constitutive equations for the description of shape memory effects in alloys. Nucl. Eng. and Des. 74, 173–182.

Cao, H., Evans, A.G., 1993. Nonlinear deformation of ferroelectric ceramics. J. Am. Ceram. Soc. 76, 890–896.

Chen, P.J., 1980. Three dimensional dynamic electromechanical constitutive relations for ferroelectric materials. International Journal of Solids and Structures 16, 1059–1067.

Chen, P.J., 1984. Hysteresis effects in deformable ceramics. In: Maugin, G.A. (Ed.), The Mechanical Behavior of Electromagnetic Solid Continua. IUTAM, Elsevier Science Publishers, pp. 137–143.

Chen, P.J., Marsden, M.M., 1981. One dimensional polar responses of the electrooptic ceramic PLZT 7/65/35 due to domain switching. Acta Mech. 41, 255–264.

Chen, P.J., Peercy, P.S., 1979. One dimensional dynamic electromechanical constitutive relations of ferroelectric materials. Acta Mech. 31, 231–241.

Chen, P.J., Tucker, T.J., 1981. Determination of the polar equilibrium properties of the ferroelectric ceramic PZT 65/35. Acta Mech. 38, 209–218.

Fatuzzo, E., Merz, W.J., 1967. Ferroelectricity. North-Holland Publishing Company, Amsterdam.

Feldtkeller, E., 1973. Dielektrische und Magnetische Materialeigenschaften, Vol. I and II. Bibliographisches Institut, Mannhein.

Fett, T., Thun, G., 1997. Determination of room-temperature tensile creep of PZT. J. Mater. Sci. Letters, submitted.

Fett, T., Müller, S., Munz, D., Thun, G., 1997. Nonsymmetry in the deformation behavior of PZT. J. Mater. Sci. Letters, submitted.

Gaudenzi, P., Bathe, K.-J., 1995. An iterative finite element procedure for the analysis of piezoelectric continua. J. Intelligent Material Systems Structures 6, 266–273.

Gong, X., 1995. Stresses near the end of an internal electrode in multilayer electrostrictive ceramic actuators. Mat. Res. Soc. Symp. Proc. 360, 83–88.

Gong, X., Suo, Z., 1996a. Reliability of ceramic multilayer actuators : a nonlinear finite element simulation. Journal of Mechanics and Physics of Solids 44, 751–769.

Gong, X., Suo, Z., 1996b. A finite element method for electrostrictive actuators : a comparison of capacitor-type and slit structures. Preprint, Mechanical and Environmental Engineering Department, Materials Department, University of California, Santa Barbara.

Haertling, G.H., 1987. PLZT electrooptic materials and applications—a review. Ferroelectrics 75, 25–55.

Hao, T.H., Gong, X., Suo, Z., 1996. Fracture mechanics for the design of ceramic multilayer actuators. Journal of Mechanics and Physics of Solids 44, 23–48.

Hom, C.L., Shankar, N., 1994. A fully coupled constitutive model for electrostrictive ceramic materials. J. Intelligent Material Systems Structures 5, 795–801.

Huo, Y., Jiang, Q., 1995. On the transformation of domain mixtures in polycrystalline ferroelectric ceramics. U.S. Office of Naval Research, Grant N00014-94-0053, Technical Report No. 6, University of Nebraska-Lincoln, Lincoln.

Hwang, S.C., Lynch, C.S., McMeeking, R. M., 1995. Ferroelectric/ferroelastic interactions and a polarization switching model. Acta Metall. Mater. 43, 2073–2084.

IRE, 1958. IRE standards on piezoelectric crystals : deformation of the elastic, piezoelectric and dielectric constants—the electromechanical coupling factor. Proc. IRE 46, 364–778.

Jaffe, B., Merz, W.J., Jaffe, H., 1971. Piezoelectric Ceramics. Academic Press, London and New York.

Jiang, Q., 1995. On the electromechanical response of electrically active materials. J. Intelligent Material Systems Structures 6, 181–190.

Kamlah M., Böhle, U., Munz, D., Tsakmakis, Ch., 1997. Macroscopic description of the non-linear electro-mechanical coupling in ferroelectrics. In : Varadan, V.V., Chandra, J. (Eds.), Smart Structures and Materials 1997 : Mathematics and Control in Smart Structures. Proceedings of SPIE 3039, 144–155.

Landau, L.D., Lifschitz, E.M., 1967. Elektrodynamik der Kontinua. Akademie Verlag, Berlin.

Loge, R.E., Suo, Z., 1996. Nonequilibrium thermodynamics of ferroelectric domain evolution. Acta Mater. 44, 3429–3438.

Lynch, C.S., 1996. The effect of uniaxial stress on the electro-mechanical response of 8/65/35 PLZT. Acta Mater. 44, 4137–4148.

Maugin, G.A., 1988. Continuum Mechanics of Electromagnetic Solids. Elsevier Science Publishers, Amsterdam.

Maugin, G.A., Pouget, J., Drouot, R., Collet, B., 1992. Nonlinear Electromechanical Couplings. John Wiley and Sons, Chichester.

Michelitsch, Th., Kreher, W., 1996. A simple model for the nonlinear material behavior of ferroelectrics. Preprint, Max-Planck-Gesellschaft, Arbeitsgruppe Mechanik heterogener Festkörper. Dresden.

Parton, V.Z., Kudryavtsev, B.A., 1988. Electromagnetoelasticity. Piezoelectrics and Electrically Conductive Solids. Gordon and Breach Science Publishers, New York.

Schäufele, A., 1996. Ferroelastische Eigenschaften von Blei-Zirkonat-Titanat-Keramiken. Dissertation, Karlsruhe 1996, Fortschritt-Berichte VDI, Reihe 5, Nr. 445, Düsseldorf.

Schäufele, A., Härdtl, K.H., 1996. Ferroelastic properties of lead zirconate titanate ceramics. J. Am. Ceram. Soc. 79, 2637–2640.

Suo, Z., 1991. Mechanics concepts for failure in ferroelectric ceramics. In : Srinivasan, A.V. (Ed.), Smart Structures and Materials, AD-Vol. 24, AMD-Vol. 123. ASME, New York, pp. 1–6.

Toupin, R.A., 1956. The elastic dielectric. J. Rational Mech. Anal. 5, 849–915.

Truesdell, C., Noll, W., 1965. The Non-Linear Field Theories of Mechanics. Handbuch der Physik, Vol. III/3, Springer Verlag, Berlin.

Yang, W., Suo, Z., 1994. Cracking in ceramic actuators caused by electrostriction. Journal of Mechanics and Physics of Solids 42, 649–663.

Zheludev, I.S., 1971. Crystalline Dielectrics. Plenum Press, New York and London.